Composites Part C: Open Access 7 (2022) 100243

Contents lists available at ScienceDirect

Composites Part C: Open Access

journal homepage: www.sciencedirect.com/journal/composites-part-c-open-access

Moisture-induced changes in the mechanical behavior of 3D printed polymers

Adedotun D. Banjo [a,c], Vinamra Agrawal [a], Maria L. Auad [b,c], Asha-Dee N. Celestine [a,c,*]

[a] Department of Aerospace Engineering, Auburn University, Auburn, AL 36849, United States of America
[b] Department of Chemical Engineering, Auburn University, Auburn, AL 36849, United States of America
[c] Center for Polymers and Advanced Composites, Auburn University, Auburn, AL 36849, United States of America

ARTICLE INFO

Keywords:
Moisture absorption
Polymer degradation
Composites
3D printing

ABSTRACT

Commonly used 3D printing polymers, such as nylon and polylactic acid (PLA), can experience significant material degradation when exposed to moisture and high temperatures for extended periods. Understanding the extent of their degradation is critical to their long term use and can also inform end-of-life strategies, such as recycling or recovery. Specimens of nylon, carbon fiber-reinforced nylon composite, and PLA, three popular 3D printing materials, were 3D printed and immersed in deionized water at 21 °C and 70 °C to evaluate the effect of moisture and temperature on their mechanical and chemical properties. Water absorption rates were much higher at elevated temperatures and, at both temperatures investigated, the nylon-based materials absorbed up to 10 times more water than PLA. A direct relationship between moisture absorption and reduction in flexural properties was observed for the nylon-based specimens, with the flexural modulus of nylon decreasing by as much as 60% after 7 days of immersion. PLA, however, displayed negligible mechanical property degradation after immersion at 21 °C, but showed substantial physical degradation after being immersed in water at 70 °C for 7 days. Analogous changes in chemical structure and crystallinity were observed via Fourier transform infrared spectroscopy and differential scanning calorimetry.

1. Introduction

Exposure to adverse environmental conditions can result in significant changes in polymer mechanical properties such as modulus, strength, and ductility [1, 2]. The most common deleterious factors include moisture, heat, ultraviolet radiation, and various chemicals [3–6]. Polymer matrix composites (PMCs) composed of continuous or short fibers bound together by a polymeric matrix can also experience several forms of degradation, especially when exposed to moisture and high-temperature environments. Moisture absorption in polymers and PMCs at ambient and elevated temperatures occurs at various rates and can result in changes in their mechanical and thermomechanical properties [7–10]. The extent to which a material may absorb moisture depends on the matrix and reinforcement material, as well as the surrounding temperature, humidity, and the length of time the material is exposed to the adverse environment [10–16].

Moisture ingress in polymers occurs via diffusion of the water molecules through the material [17–19]. The water molecules are transported to the interior of the polymers due to random molecular motions, and the rates of absorption and diffusion depend strongly on temperature and inherent moisture content. At the microscopic level, moisture diffusion is greatly influenced by the polymer's polarity and degree of crosslinking and the presence of residual monomers, hardeners, or other hydrophilic species [20–22]. Typically, moisture diffusion is characterized by an increase in material mass after exposure to a wet environment [11–13] and is modeled using Fick's law of diffusion with the temperature-dependent diffusion coefficient, D_x, [23–25]. The diffusion coefficient of compression molded polyamide 6 (nylon 6) at ambient conditions is 4.6×10^{-13} m^2/s, while that of polycarbonate and polypropylene are 6.5×10^{-12} m^2/s and 1.48×10^{-14} m^2/s, respectively [25–27]. Although various versions of Fick's model have been widely applied in the degradation kinetics of engineering thermoplastics such as nylon, polylactic acid (PLA), and acrylonitrile butadiene styrene (ABS), much work is still needed to address the onset of the degradation process which is usually observed as a decrease in the material's mechanical properties [28,29].

Nylon, a semicrystalline thermoplastic, is well known for its hygroscopicity [30,31]. The highly polar functional groups present in nylon,

* Corresponding author.
E-mail address: acelestine@auburn.edu (A.-D.N. Celestine).

https://doi.org/10.1016/j.jcomc.2022.100243

Available online 12 February 2022

such as amides, amines, and carbonyls, are responsible for its high affinity for moisture [31–34]. The molecular structure of nylon 6 is illustrated in Fig. 1a. As moisture is absorbed into nylon's amorphous regions, it first acts as a plasticizer reducing the molecular entanglements and bonding between the molecules, which results in increased volume and chain mobility and reduced glass transition temperature, T_g [10,35,36]. At elevated temperatures and after prolonged exposure to moisture, nylon degrades via hydrolysis of the amide linkages in its backbone and subsequent dissociation of the amide bonds, as well as lower molecular weight and reduced durability [37,38]. Reinforcing nylon with chopped or continuous fibers to form a nylon composite, however, tends to slow down moisture absorption as polymer chain mobility is restricted in any created free volumes [39]. Despite its affinity for moisture absorption and the resulting degradation, nylon is widely used in industrial and recreational applications because of its favorable material properties [40–43].

Polylactic acid (PLA) is a semicrystalline aliphatic polyester derived primarily from renewable resources. It is widely used in the biomedical industry for tissue engineering due to its biocompatibility and in industrial applications as bio-plastic food packaging and disposable tableware [35,44]. PLA is primarily hydrophobic [35,45] due to its methyl side groups. PLA's molecular structure is illustrated in Fig. 1b. PLA, however, can degrade under hydrolytic conditions whereby the diffusion of water molecules breaks the ester bonds. This chain scission leads to significant reductions in molecular weight and mechanical properties, although swelling is negligible [35,46,47]. Additionally, with extended exposure, small oligomers can diffuse out of the polymer leading to desorption. Studies by other researchers have revealed that PLA is relatively stable in water at moderate temperatures (15 °C–040 °C) and can absorb between 0.7 and 1 wt% water when immersed for 30 days [48] and slightly more at much longer periods of immersion [49]. Despite their hygroscopic behavior, both nylon and PLA are suitable candidate materials for fused filament deposition-based additive manufacturing and have been used extensively.

Fused deposition modeling (FDM) or 3D printing of polymeric materials is a novel technique that produces objects layer-by-layer via digitized models without the need for expensive, traditional cutting or casting machines [50–54]. A schematic of the 3D printing process is shown in Fig. 2. Pioneered more than three decades ago, this technology has traversed several fields, including the biomedical, aerospace, automotive, civil, and food industries [36, 55–62]. However, one limitation of 3D printed polymeric materials is that moisture can readily meander through the pores and layers of the final component, leading to material degradation with continued exposure. Understanding moisture-induced degradation in popular 3D printing polymers is essential to extending their use in various applications.

The objective of this work was to evaluate and compare the changes in mechanical properties of 3D printed polymers due to moisture absorption and heat. Three materials were investigated: nylon 6 (Nylon), a nylon 6 copolymer reinforced with milled carbon fibers (Nylon Composite), and PLA. The effect of immersion time and temperature on the moisture absorption behavior, mechanical and thermomechanical properties of each material was investigated. The influence of the hygroscopic nature of the polymer on the change in properties was evaluated by comparing the response of nylon and PLA. By comparing unreinforced and reinforced nylon, this work also sought to investigate the effect of the presence of additives (e.g., milled fibers) on moisture absorption and the subsequent change in properties. The degradation behavior was evaluated via mechanical testing, as well as through dynamic mechanical analysis (DMA), Fourier transform infrared spectroscopy (FTIR), and differential scanning calorimetry (DSC) analyses.

2. Materials and methods

2.1. Materials

Specimens for this study were fabricated via Fused Deposition Modeling (FDM) 3D printing. Specimens of nylon 6 (Nylon) and a nylon 6 copolymer reinforced with milled carbon fibers (Nylon Composite) were 3D printed using a Markforged MarkTwo 3D printer with Markforged's Tough Nylon and Onyx filaments, respectively. Average diameter and length of the milled carbon fibers are 7.36 μm and 108.2 μm, respectively [63]. Polylactic acid (PLA) specimens were printed using a Monoprice Maker Select V2 3D printer and Hatchbox PLA filament. Filament dimensions and print parameters are summarized in Table 1.

2.2. Moisture absorption study and diffusion coefficient

Moisture absorption analysis was performed according to ASTM standard D570 [64]. 3D printed specimens of Nylon, Nylon Composite, and PLA, with dimensions 30 × 10 × 3 mm, were first conditioned at 50 °C for 24 h. A schematic of the moisture absorption specimen is shown in Fig. 3a. After conditioning, each specimen was fully immersed in deionized (DI) water at 21 °C. Periodically, with times ranging from 30 min to 28 days, the specimens were removed, carefully dried with a paper towel, and their mass recorded using a VWR analytical balance. The percentage change in mass was then calculated using equation 1.

$$M(\%) = \frac{M_t - M_i}{M_i} \times 100 \quad (1)$$

where M is percentage moisture absorption, M_t is mass absorbed after time t (grams), and M_i is the initial mass before immersion (grams). This procedure was repeated for specimens immersed in water at 70 °C to evaluate the effect of temperature on moisture absorption. Plots of moisture absorption versus time were then generated for each material.

Each material's diffusion coefficient, D_x, was determined from a plot of normalized absorbed water versus square root time, using the slope of the initial linear region. The diffusion coefficient was then calculated as

$$D_x = \pi\left(\frac{h}{4M_{sat}}\right)^2\left(\frac{M_t}{\sqrt{t}}\right)^2 \quad (2)$$

where h is the specimen thickness (mm), M_{sat} is the saturated water

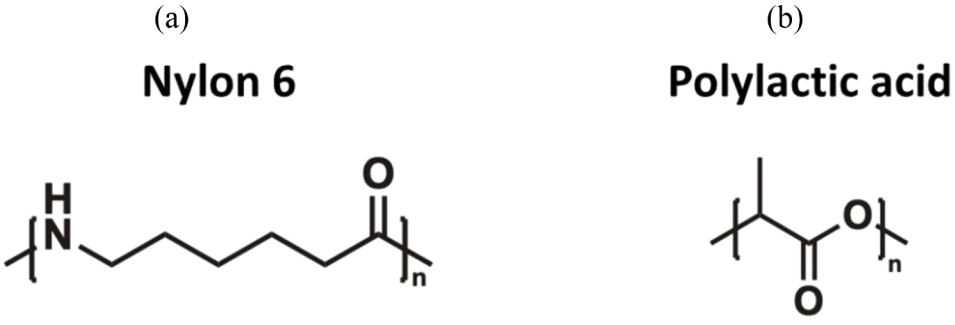

Fig. 1. Molecular structure of base polymers (a) Nylon 6 (b) Polylactic acid (PLA).

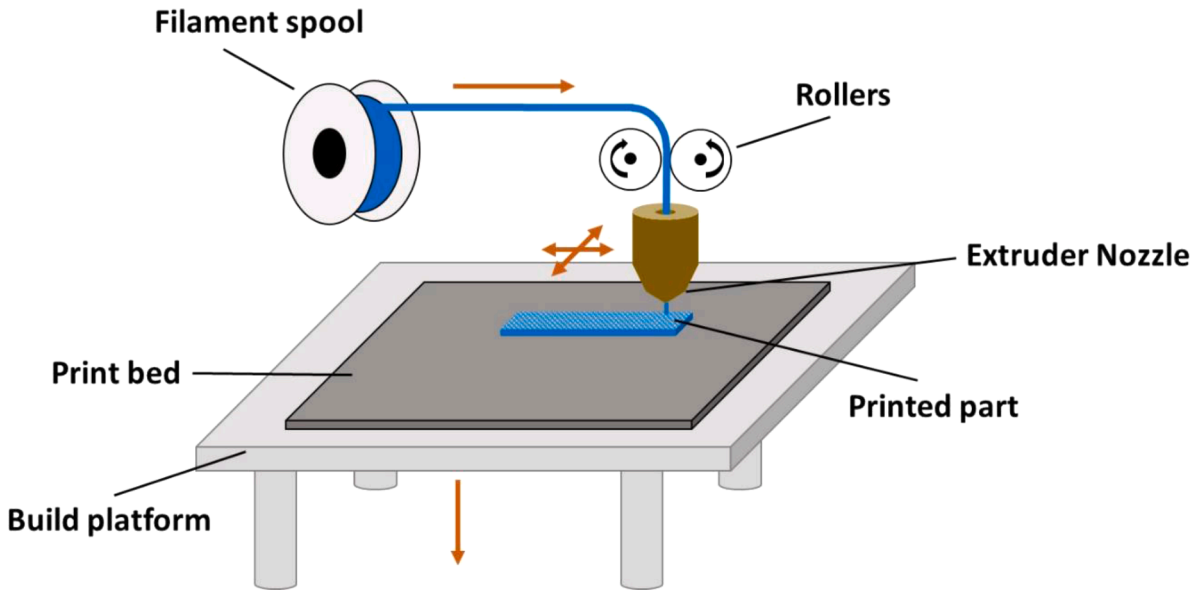

Fig. 2. Schematic of the 3D printing process.

Table 1
Printing parameters for 3D printed specimens.

Parameter	Value		
Material	Nylon	Nylon Composite	PLA
Printer	Markforged Mark Two	Markforged Mark Two	Monoprice Maker Select V2
Filament material	Tough Nylon	Onyx	Hatchbox PLA
Filament diameter (mm)	1.75	1.75	1.75
Bed temperature (°C)	N/A	N/A	60
Layer height (mm)	0.125	0.125	0.1
Print temperature (°C)	275	275	220
Infill pattern (°)	±45	±45	±45
Infill density (%)	100	100	100
Slicer software	Eiger	Eiger	Cura

content (%), and t is time (seconds).

2.3. Dynamic mechanical analysis (DMA)

A TA Instruments RSA3 dynamic mechanical analyzer was used to determine the glass transition temperature (T_g) and the storage modulus (E') of the base polymers (i.e. before immersion), according to ASTM D4065 [65]. 3D printed specimens with dimensions 30 mm x 10 mm x 3 mm were tested in 3-point bend with a 25 mm support span. Specimens were subjected to a temperature ramp of 25 °C to 100 °C, with a 5 °C/min heating rate at a frequency of 1 Hz and 0.1% maximum strain. As a result, the temperature at which the storage modulus transitioned from the glassy to the rubbery state was identified as the glass transition temperature (T_g), while the storage modulus (E') was determined as the E' value in the glassy region during the temperature ramp.

2.4. Differential scanning calorimetry (DSC) analysis

Differential scanning calorimetry (DSC) was conducted using a TA

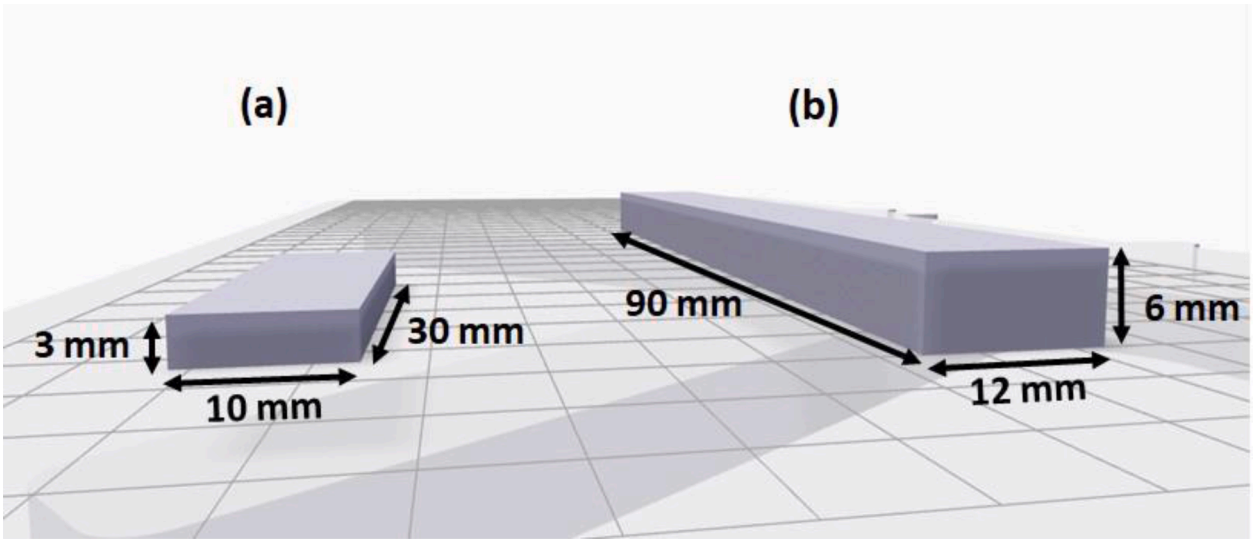

Fig. 3. Specimen schematics (a) Moisture absorption specimen (b) Flexure specimen.

Instruments DSC Q200. Heating and cooling rates of 10 °C /min (23 °C–260 °C) were used according to ASTM D7426 [66]. Virgin specimens of the base polymer, as well as specimens immersed for 7 and 14 days, were evaluated. The results were then used to determine each material's crystallization (T_c) and melting temperature (T_m). The first heating cycle was also evaluated for the three materials after moisture absorption to understand their thermal behavior with moisture ingress.

Percentage crystallinity (X_c) before and after immersion was calculated for the homogenous materials (Nylon and PLA) as

$$X_c(\%) = \frac{\Delta H_m}{\Delta H_{m100}} \times 100 \tag{3}$$

where ΔH_m is the measured enthalpy of melt, and ΔH_{m100} is the theoretical enthalpy of melting. ΔH_{m100} for nylon 6 and PLA are 190 J/g and 93 J/g, respectively [67,68]. The crystallinity of the Nylon Composite (X_{cc}) was calculated as

$$X_{cc}(\%) = \frac{\Delta H_m}{(1 - W_c)\Delta H_{m100}} \times 100 \tag{4}$$

where W_c is the weight fraction of carbon fibers in the composite, 13.43 wt%, determined via microscopic image analysis performed by Sauer [63], coupled with rule-of-mixtures calculations.

2.5. Fourier-transform infrared spectroscopy analysis

A Thermo Scientific Nicolet 6700 spectroscope fitted with a CsI attenuated total reflection (ATR) detector was used to perform Fourier transform infrared spectroscopy (FTIR) on the virgin and immersed materials according to ASTM D5477 [69]. FTIR spectra, in absorbance mode, were detected using a scanning resolution of 2 cm^{-1} and 32 scans for each specimen in the range of 4000−400 cm^{-1}. The FTIR analysis served to identify molecular vibrations and bond stretching of the bonds in both virgin and immersed specimens.

2.6. Flexural testing

Three (3)-point bend flexural tests were performed using a screw-driven Instron mechanical test frame (Model 5565, 5 kN load cell) according to ASTM standard D790 [70]. Nylon and Nylon Composite flexure specimens, with dimensions 100 × 10 × 3 mm, were fabricated using the Markforged Mark Two printer, while PLA flexure specimens measuring 90 × 12 × 6 mm were printed using the Monoprice Maker Select V2 printer. A schematic of the flexure specimen is shown in Fig. 3b. After printing, specimens were conditioned at 50 °C for 24 h, afterward they were immersed in DI water at 21 °C for specific periods. After immersion, the specimens were weighed and tested at a displacement rate of 3 mm/min with a support span of 64 mm. Specimens immersed in DI water at 70 °C were also tested. Load and displacement data were collected and used to calculate flexural stress (σ_f) and flexural strain (ε_f) according to Eqs. (5) and 6, respectively. Flexural modulus (E_f) was determined as the slope of the linear region of the flexural stress versus flexural strain plot over a strain range of 0.2%. The yield strength (σ_Y) was determined using the 0.2% strain offset method.

$$\sigma_f = \frac{3PL}{2bh^2} \tag{5}$$

$$\varepsilon_f = \frac{6\delta h}{L^2} \tag{6}$$

P denotes the applied load (N), L is the support-span (mm), b is the specimen width (mm), h is the specimen depth or thickness (mm), and δ is the maximum deflection of the beam (mm). The flexural test results were then used to evaluate the change in mechanical properties of the 3D printed specimens. Control specimens of virgin material (conditioned but not immersed) were also evaluated.

3. Results and discussion

3.1. Moisture absorption results

The effect of temperature on moisture absorption in the 3D printed materials is illustrated in Fig. 4 and summarized in Table 2. For the Nylon specimens, the maximum moisture absorbed, ~ 10 wt% occurs within the first 24 h at 21 °C, while at 70 °C the maximum moisture absorbed, ~ 7 wt%, occurs within the first 12 h, see Fig. 4a. Also, the absorption rate is significantly higher at 70 °C, with a diffusion coefficient of 5.01 × 10^{-11} m^2/s compared to 4.15 × 10^{-12} m^2/s at 21 °C. Continued immersion of the 3D printed Nylon in DI water at 70 °C results in a decrease in moisture absorbed at around 24 h, indicating desorption. For specimens immersed at 21 °C, however, moisture absorption appears to saturate before decreasing slightly.

The presence of the milled carbon fibers in the Nylon Composite resulted in a lower moisture absorption rate at 21 °C compared to that of Nylon, as seen in the slope of Fig. 4b and the diffusion coefficient in Table 2. This result indicates the decelerating effect of the milled carbon fibers on moisture absorption into the host polymer. However, the maximum moisture absorbed by the nylon matrix within the composite at this temperature was about the same as that of the Nylon specimens, at ~ 9.5 wt%, although it was attained after a slightly longer period. Therefore, the milled fibers only served to slow down the ingress of water and had little effect on the total amount of moisture absorbed over time, possibly due to their small size (≈ 108 um) and low weight fraction (13.4 wt%). At the elevated temperature of 70 °C, the moisture absorption rate in the Nylon Composite was lower than that of the Nylon, although not as much as was observed at 21 °C, illustrating the significant effect of temperature on diffusion. Here, the maximum moisture absorbed was ~ 7 wt%.

These results confirm nylon's high affinity for moisture, with absorption rates influenced by temperature changes as more energy is available at higher temperatures [29]. The presence of the non-hygroscopic fibers in the Nylon Composite reduces the moisture absorption rate as the fibers restrict the movement of water molecules [29,71]. With increased water content in the Nylon specimens, chain scission occurs, enabling small oligomers to diffuse out of the polymer leading to desorption [10].

The PLA specimens absorb ~ 0.9 wt% moisture at 21 °C after 24 h, which then remains relatively constant for the next 10 days, see Fig. 4c. At 70 °C, the maximum moisture absorbed by the PLA specimens was 0.7 wt%. However, the absorbed moisture then decreased significantly after 10 days indicating material desorption. The diffusion coefficient at 21 °C was the same order of magnitude as that for the nylon-based materials. However, it was significantly lower at 70 °C. The difference in absorption response between nylon and PLA can be attributed to the absence of polar groups in PLA, which are known to be largely responsible for the enhanced moisture absorption behavior of nylon. It has also been observed that PLA undergoes bulk degradation when immersed in water at elevated temperatures [72]. These results are in agreement with those found in the literature [46]. While the Nylon and Nylon Composite specimens were still intact after 28 days of immersion, the PLA specimens showed signs of significant material degradation. They were very fragile physically after 7 days at 70 °C.

Thermal and thermomechanical properties of the base (virgin) polymers are also included in Table 2. Here, we observe the subtle yet critical differences in each material's response to increased temperature. The storage modulus (E') of PLA is twice that of nylon and its glass transition temperature (T_g) is much closer to the elevated immersion temperature, 70 °C. Crystallization and melting temperatures are also different. These characteristics undoubtedly affect the response of the 3D printed materials after prolonged immersion.

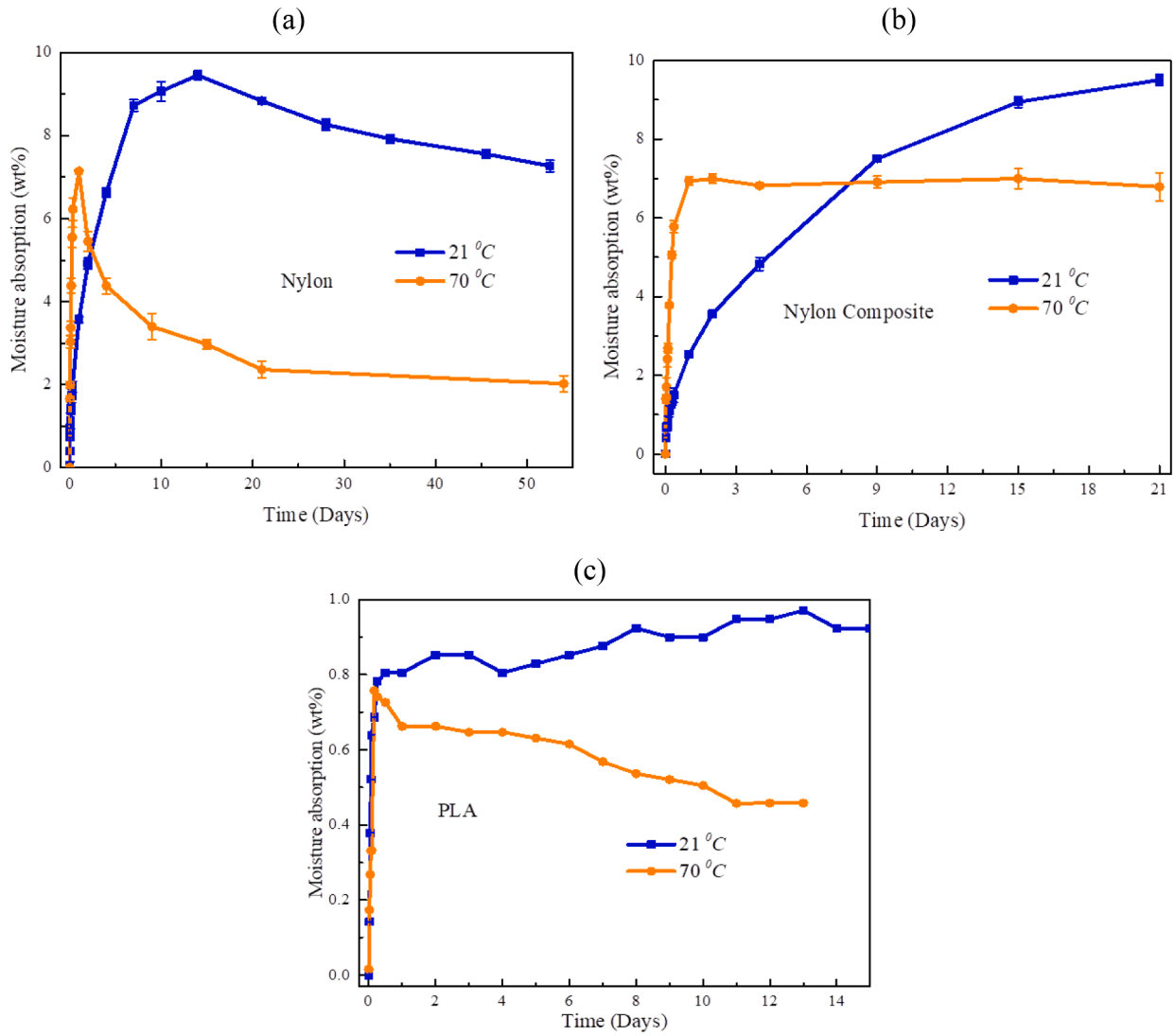

Fig. 4. Moisture absorption behavior of 3D printed materials after immersion in DI water (a) Nylon (b) Nylon Composite (c) PLA.

Table 2
Moisture absorption and thermomechanical response of base (virgin) polymers.

Parameters		Material Nylon	Nylon Composite	PLA
Diffusion Coefficient, D_x (m^2/s)	21 °C	4.17×10^{-12}	1.61×10^{-12}	5.73×10^{-12}
	70 °C	5.01×10^{-11}	3.37×10^{-11}	1.55×10^{-12}
Maximum moisture absorbed (wt%)	21 °C	10.0	9.5	0.9
	70 °C	7.0	7.0	0.7
Storage modulus, E' (GPa)		1.14	1.67	2.20
Glass transition temperature, T_g (°C)		36.1	37.1	68.6
Crystallization temperature, T_c (°C)		156.5	162.7	103.7
Melting temperature, T_m (°C)		222.8	200.3	175.1

3.2. Changes in crystallinity

Each material's response to heating was evaluated via differential scanning calorimetry (DSC). Representative DSC plots are shown in Fig. 5. The degree of crystallinity in each of the three semicrystalline materials was calculated based on their enthalpy of melting and then used to evaluate the effect of elevated temperature and moisture on the crystalline phases within the first 14 days of immersion. The results are summarized in Table 3. For the Nylon specimens immersed in DI water at 21 °C, the percentage crystallinity decreased from approximately 22% to 12% after 14 days, indicating a moisture-induced breakdown of the molecular chains in both the amorphous and crystalline regions of the polymer, see Table 3a. During the moisture absorption process, water first agglomerates in the easy-to-penetrate amorphous regions [73] as diffusion into the crystalline phase is a bit more difficult in the early stages [74] and only occurs after prolonged immersion, with potential decreases in crystallinity. From the results, 7 days of immersion is sufficient time for the water molecules to enter and disrupt the crystalline regions. As discussed earlier, elevated temperatures can aid moisture diffusion into the crystalline phase. This is observed with the Nylon specimens immersed in DI water at 70 °C where the percentage crystallinity decreases to ~11% after 14 days of immersion. The intermolecular hydrogen bonds are more energized with higher temperatures, allowing the water molecules to permeate into the crystalline phase more readily, reducing crystallinity after immersion [75].

The degree of crystallinity in the Nylon Composite immersed at 21 °C also decreased with time. The composite material, however, was able to retain a slightly higher crystallinity after 14 days compared to the plain

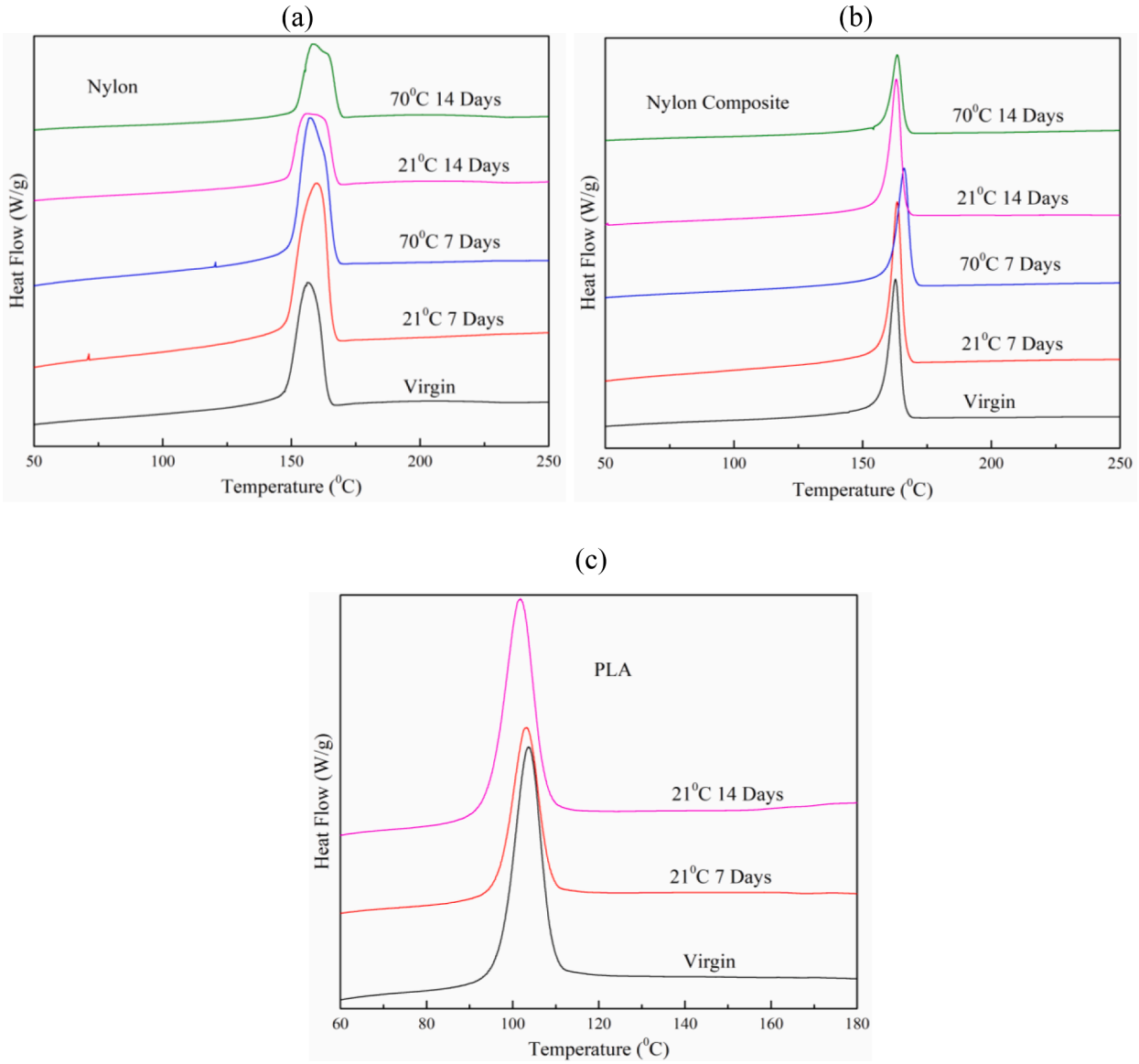

Fig. 5. Differential Scanning Calorimetry (DSC) plots of the 3D printed material after immersion in DI water at 21 °C and 70 °C (a) Nylon (b) Nylon Composite (c) PLA.

nylon material which may be attributed to the presence of the milled fibers. At 70 °C, these embedded milled fibers do not provide as much advantage as the crystallinity of the composite is shown to be significantly reduced after 14 days, just as with the Nylon specimens. This response is possibly due to heat- and moisture-induced degradation of the fiber-matrix interface, in addition to matrix degradation [29]. At this temperature, the absorbed hot water permeates easily throughout the crystalline regions causing molecular degradation.

The percentage crystallinity for the PLA specimens immersed at 21 °C decreased from 41% to 35% after 7 days, but then increased to 53% crystallinity after 14 days. Although the absorbed moisture content in PLA was lower than that of the nylon-based specimens (~1 wt%), the water molecules that were able to penetrate the matrix within the first week were successful at disrupting the crystalline regions within the PLA polymer. The increase in crystallinity after two weeks suggests significant deterioration of the amorphous regions. Indeed, these specimens were very brittle and fragile at this point. After 7 days at 70 °C, the physical condition of the PLA specimens was degraded to the extent that accurate DSC measurements could not be obtained. The disparate response of PLA can be attributed to its molecular structure, namely the absence of the polar amide groups. Overall, these changes in crystallinity for both the nylon-based materials and PLA highlight the importance of regulating environmental conditions to ensure 3D printed components and prototypes do not degrade prematurely.

3.3. Fourier transform infrared spectroscopy (FTIR)

Changes in chemical bonding and functional groups after immersion in DI water were evaluated via FTIR. Fig. 6 shows the FTIR spectra for the three materials before and after immersion at 21 °C and 70 °C for 14 days. For the virgin Nylon, the peak at 591 cm^{-1} represents the O=C—N bending, while the peak at 931 cm^{-1} is the C—C bond stretching, see Fig. 6a. Peaks at 1345, 1542, 1663 cm^{-1} can be assigned to the amide I, II, and III bonds, respectively [76]. Peaks at 2856 and 2968 cm^{-1} are symmetric and asymmetric CH_2 bonds, while the 3320 cm^{-1} peak represents the N—H bonds deforming. During immersion in DI water, the water molecules enter between the layers of the 3D printed material and diffuse into the polymer and between the molecular chains. When this occurs, it results in shifts in peak location and increases in peak intensity. The penetration path of the water is facilitated by the creation of

Table 3

a. Differential scanning calorimetry (DSC) results for specimens immersed in DI water at 21 °C.

Material	Immersion Time (days)	T_c (°C)	ΔH_m (J/g)	X_c (%)
Nylon	0 (Control)	156.5	41.1	21.7
	7	160.1	37.8	19.9
	14	157.1	23.3	12.3
Nylon Composite	0 (Control)	162.7	36.6	22.3
	7	163.5	30.0	18.2
	14	163.1	26.8	16.3
PLA	0 (Control)	103.7	38.4	41.2
	7	103.2	32.1	34.6
	14	101.8	49.2	52.9

Table 3b. Differential scanning calorimetry (DSC) results for specimens immersed in DI water at 70 °C.

Material	Immersion Time (days)	T_c (°C)	ΔH_m (J/g)	X_c (%)
Nylon	7	157.4	36.1	19.0
	14	158.8	20.2	10.6
Nylon Composite	7	166.1	22.2	13.5
	14	163.4	15.5	9.41

T_c – crystallization peak temperature measured in cooling.
ΔH_m – experimental enthalpy of melting.
X_c – percentage crystallinity.

free volume in the polymer as it reacts with the water [77]. For the specimens immersed at 21 °C, the result is a slight shift in peak location of the O=C—N and C—C bonds to 598 and 933 cm^{-1}, respectively, while the new locations of the amide I, II and III bonds are 1348, 1545 and 1667 cm^{-1}, respectively. After 14 days at 70 °C, the O=C—N bending shifts to 600 cm^{-1} and the C—C bond shifts to 935 cm^{-1}. The amide I, II and III bonds have also shifted to 1353, 1550 and 1671 cm^{-1}, respectively.

The FTIR spectra for the Nylon Composite before and after immersion in DI water for 14 days are shown in Fig. 6b. The spectrum of the virgin Nylon Composite material is essentially the same as that for the virgin Nylon in Fig. 6a, as nylon is the matrix polymer in both materials. As with Nylon, changes in peak intensity and locations are observed after 14 days of immersion in DI water, at both temperatures investigated, because of the effect of the water molecules on the nylon matrix. The presence of the milled carbon fibers (length ≈ 108 μm) does not appear to significantly impact the water-induced changes in chemical bonding.

The spectrum for the virgin PLA (Fig. 6c) indicates the presence of C—O asymmetrical stretching with peaks at 1074, 1130 and 1185 cm^{-1} and C—H bending at 1462 cm^{-1}. In addition, a band of C=O stretching is observed around 1753 cm^{-1} and CH stretching at 2833 and 2907 cm^{-1} [46,78]. After immersion in DI water for 14 days at 21 °C, an increase in

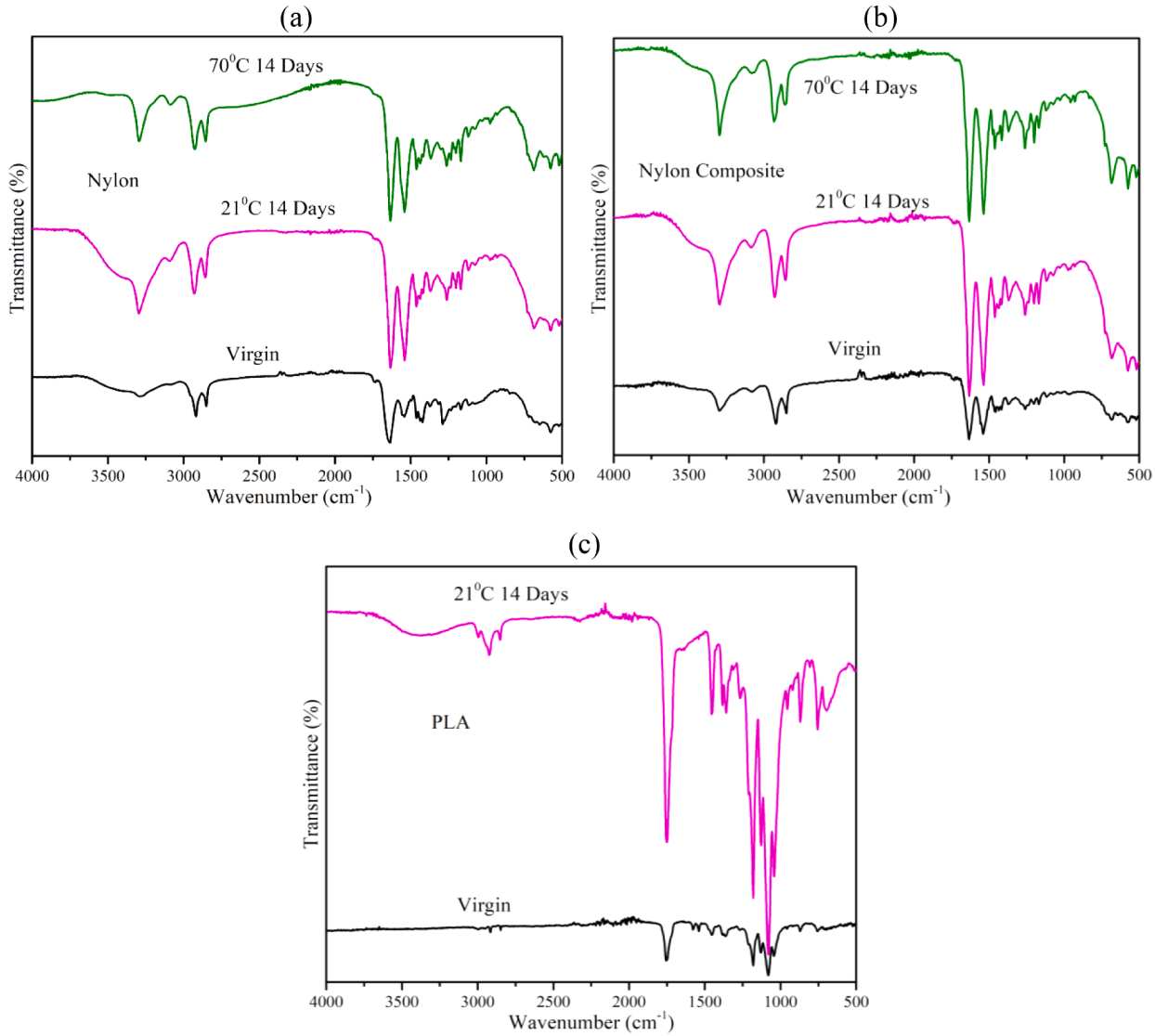

Fig. 6. FTIR spectra of specimens immersed in DI water at 21 °C and 70 °C (a) Nylon (b) Nylon Composite (c) PLA (21 °C only).

peak intensity is observed but with only small changes in peak locations. This behavior can be attributed to the absence of the polar amide groups that are prevalent in the nylon-based materials.

3.4. Mechanical behavior of 3D printed materials

The mechanical response of the 3D printed materials immersed in DI water was evaluated via flexural testing. Representative flexural stress versus flexural strain plots for the virgin material and for specimens immersed at 21 °C and 70 °C for one (1) day are shown in Fig. 7. Each material exhibits linear elastic behavior followed by yielding, although the degree of yielding is much lower in the more brittle PLA. As expected, virgin specimens withstood the largest flexural stresses. As the amount of water absorbed by the nylon matrix increased, both the modulus and strength decreased as depicted by the reduced slopes and stresses, respectively. These decreases are due to plasticization of the host nylon polymer, leading to increased chain mobility and degradation of the polymer chains. The Nylon Composite specimens showed similar changes in mechanical behavior at both 21 °C and 70 °C, with the specimens immersed at 70 °C experiencing significant decreases in strength and modulus. Only small changes in mechanical response are observed for the PLA specimens after immersion in DI water. This is not surprising, as PLA was the least hygroscopic of the three materials evaluated, absorbing only ~0.9 wt% water after extended immersion.

3.5. Flexural yield strength and flexural modulus

Initial flexural yield strength and flexural modulus of the virgin materials are shown in Table 4. In contrast, the flexural yield strength and flexural modulus of the three materials after immersion in DI water are summarized in Figs. 8 and 9, respectively. Virgin PLA displayed the highest yield strength and modulus, followed by the virgin Nylon Composite and then virgin Nylon. Within the first 24 h, the change in

Table 4
Flexural yield strength and flexural modulus of virgin 3D printed materials.

Property	Material Nylon	Nylon Composite	PLA
Flexural Yield Strength, σ_Y (MPa)	13.4	28.1	47.5
Flexural Modulus, E_f (MPa)	774.2	1540.4	1780.8

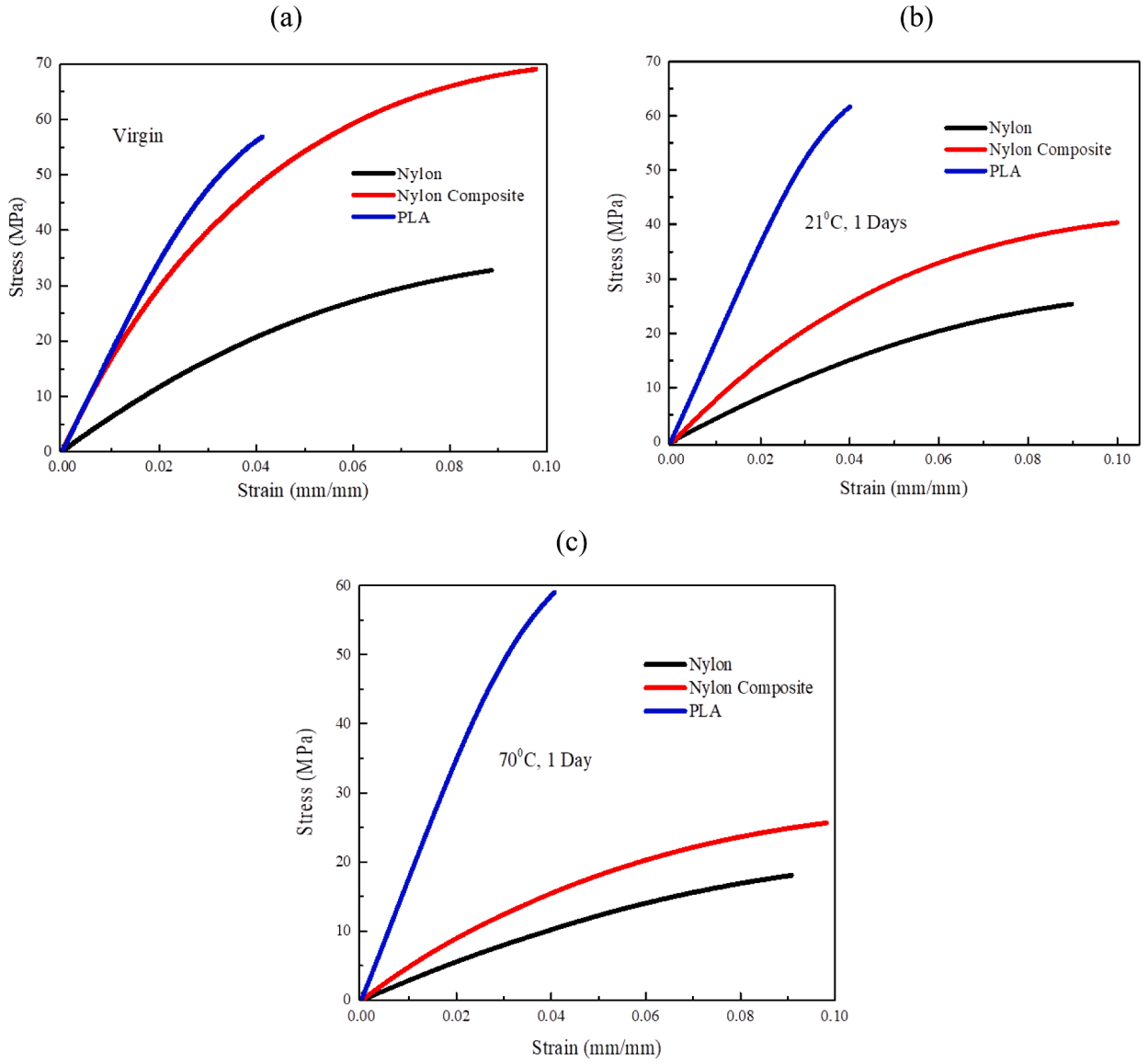

Fig. 7. Representative flexural stress versus flexural strain plots for 3D printed specimens immersed in DI water. (a) Virgin material (b) Immersed in DI water at 21 °C for 1 day (c) Immersed in DI water at 70 °C for 1 day.

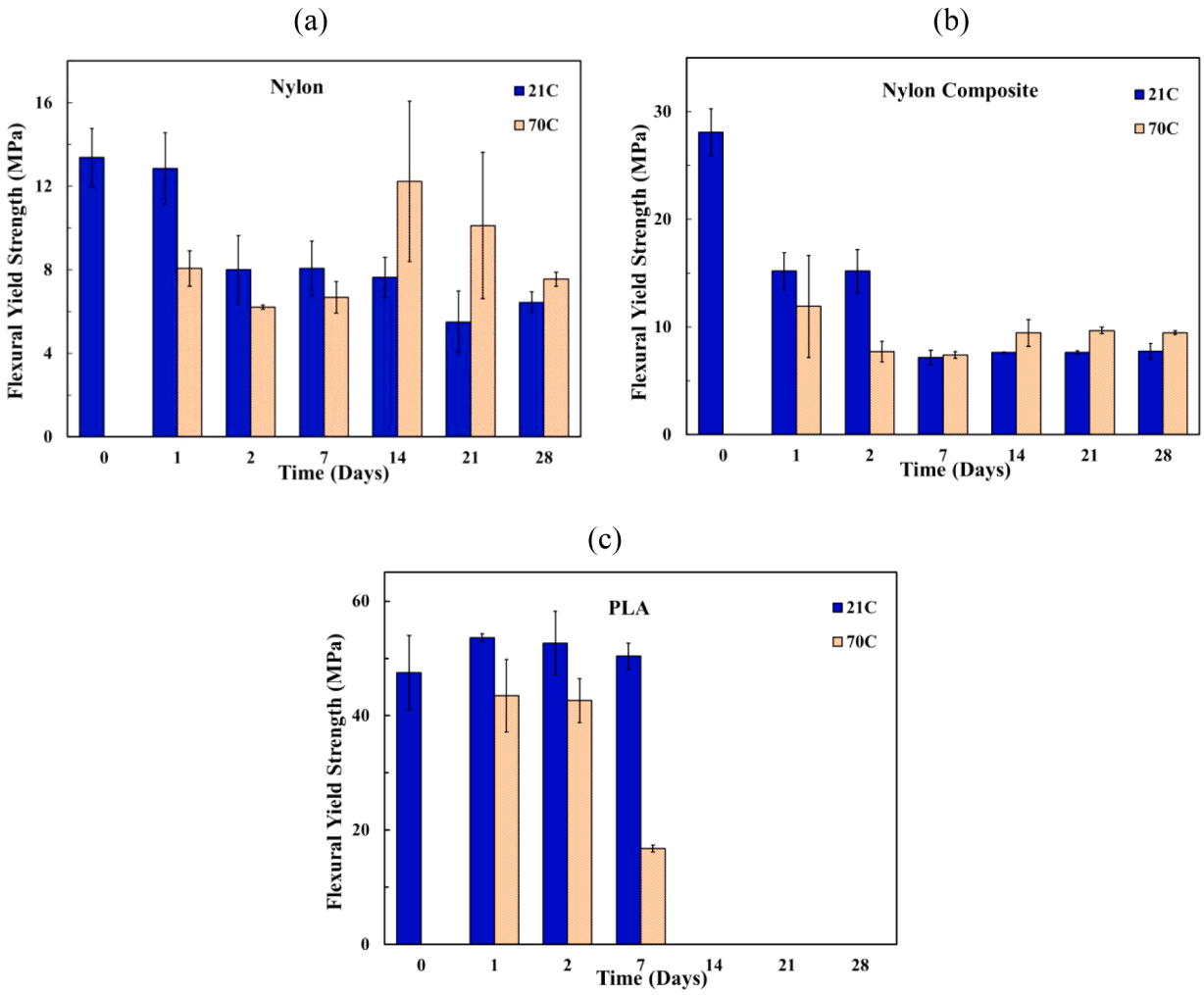

Fig. 8. Flexural yield strength (σ_Y) of 3D printed materials after immersion in DI water at 21 °C and 70 °C (a) Nylon (b) Nylon Composite (c) PLA. Error bars reflect one standard deviation of data.

yield strength of the Nylon specimens immersed in DI water at 21 °C was small at approximately 4%, see Fig. 8a. However, after continued immersion (2 days and beyond), the strength decreased to ~ 40% of its initial value and by as much as 59% (5.5 MPa) after 21 days. This trend of significantly decreasing yield strength can be attributed to the intermolecular reactions between the water and nylon molecules, plasticization, as well as molecular breakdown and is similar to that observed by Ishak et al. in their study of the effect of hydrothermal conditioning on carbon fiber reinforced nylon [1]. For Nylon specimens immersed at 70 °C, a dramatic reduction in yield strength was observed much sooner, with a 40% decrease occurring after just 1 day of immersion. The yield strength of these specimens continued to decrease until the 2-week (14-day) mark, with a maximum 54% reduction which was then followed by an increase in yield strength before falling to 7.6 MPa after 28 days. This progression of mechanical behavior at 70 °C can be attributed to decreased specimen water content (desorption) which manifests as temporary yield strength recovery. With continued immersion, however, strength decreases again as hydrolysis and desorption progress within the polymer.

The Nylon Composite specimens lose as much as ~75% of their initial yield strength after immersion in DI water for 7 days, exhibiting a larger change in mechanical response than the Nylon specimens within the same timeframe (see Fig. 8b). This behavior was unexpected as it was initially hypothesized that the milled carbon fibers' presence would help retain mechanical strength for a longer period. Researchers working with this nylon composite material have, however, observed poor fiber-matrix adhesion, as well as inadequate bonding between the 3D-printed layers in the virgin material [79–81]. We believe that the absorbed water molecules degraded the matrix polymer, and further degraded the adhesion between the milled fiber and matrix, and also between the specimen layers, leading to a more drastic decrease in mechanical properties; a phenomenon also observed by other researchers [29]. Significant decreases in yield strength were also observed with continued immersion in DI water, at both temperatures evaluated. The mechanical response of the 3D printed polymers are in good agreement with the tensile property changes observed by several researchers including Fang et al. and Ma and co-workers [2,28,82].

PLA did not exhibit considerable changes in strength after immersion at 21 °C, with values remaining around 50 MPa and increasing slightly with extended immersion, see Fig. 8c. Immersion in DI water at 70 °C for 2 days and less did not result in the drastic decreases in strength that were expected considering that 70 °C is close to PLA's glass transition temperature. After 7 days of immersion at 70 °C, however, a significant reduction in strength was observed, indicating significant mechanical degradation. PLA specimens immersed in DI water at 70 °C beyond 7 days were also physically degraded, and as such, their mechanical properties could not be reliably attained.

Changes in flexural modulus were parallel to those observed for flexural yield strength, see Fig. 9. Over 28 days of immersion at 21 °C, both Nylon and Nylon Composite specimens exhibited large reductions in modulus, from 25% to as much as 72%. At the elevated temperature, 70 °C, reductions in modulus were approximately 60% after only one

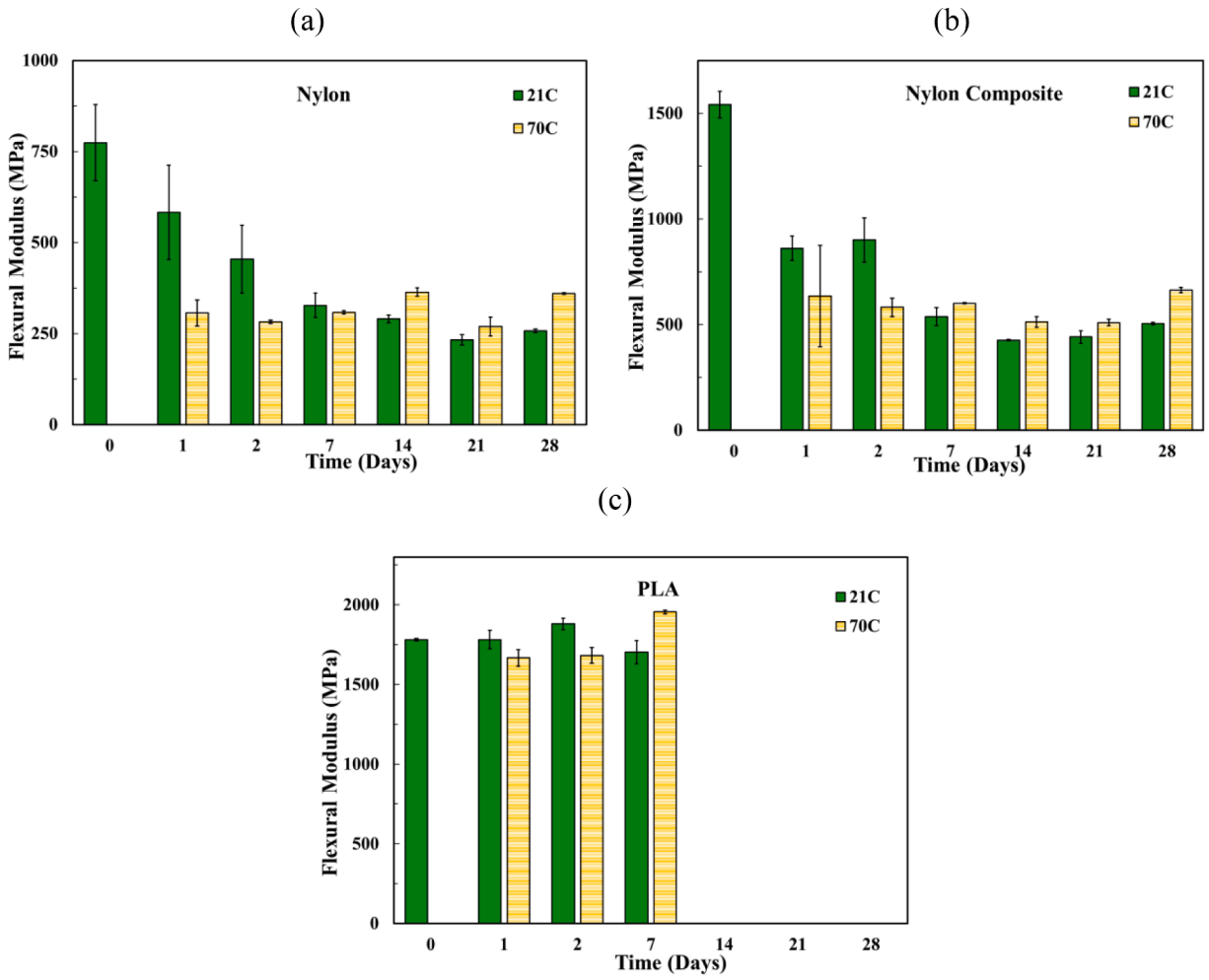

Fig. 9. Flexural modulus (E_f) of 3D printed materials after immersion in DI water at 21 °C and 70 °C (a) Nylon (b) Nylon Composite (c) PLA. Error bars reflect one standard deviation of data.

day of immersion. The changes in modulus for PLA immersed at 21 °C were comparable with the changes in yield strength, with small changes in the first 7 days before the physical disintegration of the specimens. The influence of elevated temperature on modulus was moderate in PLA with a maximum decrease of 6%. Again, the absence of polar amide groups in PLA, which renders it less hygroscopic than the nylon-based materials, is the likely explanation for this difference in mechanical response between the material groups.

The results of this work illustrate the importance of molecular structure and material composition on the mechanical response of popular 3D printing materials, especially when they are exposed to moisture and elevated temperatures for extended periods. Understanding the degree of mechanical property degradation can help in the design of components which are recyclable and/or recoverable at the end of their useful life. These degradation characteristics can also be used to enhance constitutive mechanical property degradation models such as the one described in the work by Celestine et al. [28].

4. Conclusions

This study investigated the effects of moisture and temperature on the behavior of three commonly used 3D printing semicrystalline polymers: nylon, a fiber-reinforced nylon composite, and polylactic acid (PLA). 3D printed specimens of each material were immersed in DI water at 21 °C and 70 °C, and changes in their chemical and mechanical behavior were evaluated. The three materials experienced different degrees of degradation, which were closely related to their unique molecular structure and hygroscopic nature. As expected, exposure to moisture at elevated temperatures resulted in an increased absorption rate. The Nylon and Nylon Composite both attained a maximum moisture content of ~ 10 wt% after only 24 h of immersion, while the PLA specimens absorbed approximately ~ 0.9 wt% within the same period. While the moisture absorption was more rapid at elevated temperatures, the maximum amount absorbed at 70 °C was lower than that for specimens immersed at 21 °C. The absorbed water molecules were able to penetrate both the amorphous and crystalline regions leading to reductions in the degree of crystallinity. The influence of both chemical structure (Nylon versus PLA) and additives (Nylon versus Nylon Composite) is evident in these results.

Plasticization and eventual hydrolytic cleavage due to moisture absorption resulted in significant losses in mechanical properties. Flexural yield strength and modulus were both adversely affected by the absorbed moisture, with the most significant reductions observed for specimens immersed at 70 °C. These changes in chemical and mechanical behavior provide a framework for understanding the effect of long term heat and moisture exposure on the material behavior of popular 3D printing materials. The results can also be used to refine degradation kinetics models and aid in the development of sustainable 3D printed polymers and polymer matrix composites.

Declaration of Competing Interest

The authors declare that they have no known competing financial interests or personal relationships that could have appeared to influence the work reported in this paper.

Acknowledgments

The authors acknowledge the support of Dr. Ramsis Farag and Dr. Nima Alizadeh at the Center for Polymers and Advanced Composites at Auburn University for assistance with mechanical and thermal characterization. AB and AC acknowledge financial support from the Department of Aerospace Engineering at Auburn University.

References

[1] Z.A.M. Ishak, J.P. Berry, Hygrothermal aging studies of short carbon fiber reinforced nylon 6.6, J. Appl. Polym. Sci. 51 (13) (1994) 2145–2155.
[2] L. Fang, et al., Effects of environmental temperature and humidity on the geometry and strength of polycarbonate specimens prepared by fused filament fabrication, Materials 13 (19) (2020) 4414.
[3] E.H. Backes, et al., Analysis of the Degradation during melt processing of PLA/Biosilicate® composites, J. Composites Sci. 3 (2) (2019) 52.
[4] R.M. Rowell, Handbook of Wood Chemistry and Wood Composites, CRC Press, 2012.
[5] F. Xie, et al., Degradation and stabilization of polyurethane elastomers, Prog. Polym. Sci. 90 (2019) 211–268.
[6] B.G. Achhammer, F.W. Reinhart, G.M. Kline, Mechanism of the degradation of polyamides, J. Appl. Chem. 1 (7) (1951) 301–320.
[7] S.G. Prolongo, M.R. Gude, A. Ureña, Water uptake of epoxy composites reinforced with carbon nanofillers, Composites Part A 43 (12) (2012) 2169–2175.
[8] N.-.M. Barkoula, Environmental Degradation of Carbon Nanotube Hybrid Aerospace composites, in Carbon Nanotube Enhanced Aerospace Composite Materials, Springer, 2013, pp. 337–376.
[9] C. Yang, et al., A comprehensive review on water diffusion in polymers Focusing on the Polymer–Metal Interface Combination, Polymers 12 (1) (2020) 138.
[10] C.-.H. Shen, G.S. Springer, Moisture absorption and desorption of composite materials, J. Compos. Mater. 10 (1) (1976) 2–20.
[11] Y.J. Weitsman, M. Elahi, Effects of fluids on the deformation, strength and durability of polymeric composites – an overview, Mechanics of Time-Dependent Materials 4 (2) (2000) 107–126.
[12] Y. Weitsman, Comprehensive composite materials, Polym. Matrix Composites 2 (2000).
[13] D. Choqueuse, et al., Aging of composites in water: comparison of five materials in terms of absorption kinetics and evolution of mechanical properties. High Temperature and Environmental Effects On Polymeric Composites: 2nd Volume, ASTM International, 1997.
[14] M.C. Gupta, V.G. Deshmukh, Thermal oxidative degradation of poly-lactic acid, Colloid Polym. Sci. 260 (3) (1982) 308–311.
[15] T.W. Clyne, D. Hull, An Introduction to Composite Materials, Cambridge University Press, 2019.
[16] S. Joseph, et al., Mechanical properties and water sorption behavior of phenol–formaldehyde hybrid composites reinforced with banana fiber and glass fiber, J. Appl. Polym. Sci. 109 (3) (2008) 1439–1446.
[17] G. Marom, L.J. Broutman, Moisture in Epoxy Resin Composites, J. Adhes. 12 (2) (1981) 153–164.
[18] C. Williams, Effect of Water Absorption On the Room Temperature Properties of Carbon Fiber and Glass Fiber Reinforced Polymer Composites, Ship Materials Engineering Department, David Taylor Research Center, 1998. DTRC/SME-88-85, December.
[19] M. Fincan, Assessing Viscoelastic Properties of Polydimethylsiloxane (PDMS) Using Loading and Unloading of the Macroscopic Compression test. Thesis, University of South Florida, 2015.
[20] F.A. Ramirez, L.A. Carlsson, B.A. Acha, Evaluation of water degradation of vinylester and epoxy matrix composites by single fiber and composite tests, J. Mater. Sci. 43 (15) (2008) 5230–5242.
[21] D.-.W. Suh, et al., Equilibrium water uptake of epoxy/carbon fiber composites in hygrothermal environmental conditions, J. Compos. Mater. 35 (3) (2001) 264–278.
[22] J. George, S.S. Bhagawan, S. Thomas, Effects of environment on the properties of low-density polyethylene composites reinforced with pineapple-leaf fibre, Compos. Sci. Technol. 58 (9) (1998) 1471–1485.
[23] A. Fick, Ueber diffusion, Ann Phys 170 (1) (1855) 59–86.
[24] Xuejun, F. Mechanics of moisture for polymers: fundamental concepts and model study. in EuroSimE 2008 - International Conference On Thermal, Mechanical and Multi-Physics Simulation and Experiments in Microelectronics and Micro-Systems. 2008.
[25] L. Monson, M. Braunwarth, C.W. Extrand, Moisture absorption by various polyamides and their associated dimensional changes, J. Appl. Polym. Sci. 107 (1) (2008) 355–363.
[26] P.S. Nasirabadi, M. Jabbari, J.H. Hattel, Estimation of water diffusion coefficient into polycarbonate at different temperatures using numerical simulation, AIP Conf Proc 1738 (1) (2016), 030045.
[27] H. Chandekar, et al., Effect of chemical treatment on mechanical properties and water diffusion characteristics of jute-polypropylene composites, Polym Compos 41 (4) (2020) 1447–1461.
[28] A.-D.N. Celestine, V. Agrawal, B. Runnels, Experimental and numerical investigation into mechanical degradation of polymers, Compos. Part B 201 (2020), 108369.
[29] I. Ksouri, O. De Almeida, N. Haddar, Long term ageing of polyamide 6 and polyamide 6 reinforced with 30% of glass fibers: physicochemical, mechanical and morphological characterization, J. Polym. Res. 24 (8) (2017) 133.
[30] T. Trimaille, et al., Novel polymeric micelles for hydrophobic drug delivery based on biodegradable poly(hexyl-substituted lactides), Int. J. Pharm. 319 (1) (2006) 147–154.
[31] L. Monson, M. Braunwarth, C. Extrand, Moisture absorption by various polyamides and their associated dimensional changes, J. Appl. Polym. Sci. 107 (1) (2008) 355–363.
[32] C.J. Verbeek, L.E. Berg, Recent developments in thermo-mechanical processing of proteinous bioplastics, Recent Patents Mater. Sci. 2 (3) (2009) 171–189.
[33] A.K. Ghosh, M. Dwivedi, Processability of thermoplastic composites. Processability of Polymeric Composites, Springer, 2020, pp. 151–177.
[34] P. Thanki, Photo-oxidative Degradation and Stabilization of Nylon 66 in Presence of Acid Blue dyes. Thesis, University of Pune, 1999.
[35] T. Casalini, et al., A perspective on polylactic acid-based polymers use for nanoparticles synthesis and applications, Front. Bioeng. Biotechnol. 7 (259) (2019).
[36] J.W. Stansbury, M.J. Idacavage, 3D printing with polymers: challenges among expanding options and opportunities, Dent. Mater. 32 (1) (2016) 54–64.
[37] E.O. Ogunsona, M. Misra, A.K. Mohanty, Accelerated hydrothermal aging of biocarbon reinforced nylon biocomposites, Polym. Degrad. Stab. 139 (2017) 76–88.
[38] H. Miyamoto, IUPAC-NIST solubility data series. 84. Solubility of inorganic actinide compounds, J. Phys. Chem. Ref. Data 36 (4) (2007) 1417–1736.
[39] M.A. Masuelli, Introduction of fibre-reinforced polymers– polymers and composites: concepts, properties and processes. Fiber Reinforced Polymers-The Technology Applied For Concrete Repair, IntechOpen, 2013.
[40] J.L. Thomason, The influence of fibre length, diameter and concentration on the modulus of glass fibre reinforced Polyamide 6,6, Compos. Part A 39 (11) (2008) 1732–1738.
[41] N.G. Karsli, A. Aytac, Tensile and thermomechanical properties of short carbon fiber reinforced polyamide 6 composites, Compos. Part B 51 (2013) 270–275.
[42] N. Jia, V.A. Kagan, Effects of time and temperature on the tension-tension fatigue behavior of short fiber reinforced polyamides, Polym. Compos. 19 (4) (1998) 408–414.
[43] S. Mortazavian, A. Fatemi, Effects of fiber orientation and anisotropy on tensile strength and elastic modulus of short fiber reinforced polymer composites, Compos. Part B 72 (2015) 116–129.
[44] I. Vroman, L. Tighzert, Biodegradable Polymers, Materials 2 (2) (2009) 307–344.
[45] T. Ouchi, Y. Ohya, Design of lactide copolymers as biomaterials, J. Polym. Sci. Part A Polym. Chem. 42 (3) (2004) 453–462.
[46] G.H. Yew, et al., Water absorption and enzymatic degradation of poly(lactic acid)/rice starch composites, Polym. Degrad. Stab. 90 (3) (2005) 488–500.
[47] R.M. Taib, et al., Properties of kenaf fiber/polylactic acid biocomposites plasticized with polyethylene glycol, Polym. Compos. 31 (7) (2010) 1213–1222.
[48] G.W. Melenka, et al., Evaluation and prediction of the tensile properties of continuous fiber-reinforced 3D printed structures, Compos. Struct. 153 (2016) 866–875.
[49] L. Li, et al., Composite modeling and analysis for fabrication of FDM prototypes with locally controlled properties, J. Manuf. Process. 4 (2) (2002) 129–141.
[50] S.A. Hinchcliffe, K.M. Hess, W.V. Srubar, Experimental and theoretical investigation of prestressed natural fiber-reinforced polylactic acid (PLA) composite materials, Compos. Part B 95 (2016) 346–354.
[51] R.T.L. Ferreira, et al., Experimental characterization and micrography of 3D printed PLA and PLA reinforced with short carbon fibers, Compos. Part B 124 (2017) 88–100.
[52] J. Justo, et al., Characterization of 3D printed long fibre reinforced composites, Compos. Struct. 185 (2018) 537–548.
[53] Z. Hou, et al., 3D printed continuous fibre reinforced composite corrugated structure, Compos. Struct. 184 (2018) 1005–1010.
[54] L.E. Murr, Frontiers of 3D printing/additive manufacturing: from human organs to aircraft fabrication, J. Mater. Sci. Technol. 32 (10) (2016) 987–995.
[55] M. Talagani, et al., Numerical simulation of big area additive manufacturing (3D printing) of a full size car, SAMPE J. 51 (4) (2015) 27–36.
[56] N. Labonnote, et al., Additive construction: state-of-the-art, challenges and opportunities, Autom. Constr. 72 (2016) 347–366.
[57] J.I. Lipton, et al., Additive manufacturing for the food industry, Trends Food Sci. Technol. 43 (1) (2015) 114–123.
[58] B. Berman, 3-D printing: the new industrial revolution, Bus Horiz. 55 (2) (2012) 155–162.
[59] R. Melnikova, A. Ehrmann, K. Finsterbusch, 3D printing of textile-based structures by Fused Deposition Modelling (FDM) with different polymer materials, IOP Conf. Ser. 62 (2014), 012018.
[60] Q. Sun, et al., Effect of processing conditions on the bonding quality of FDM polymer filaments, Rapid Prototyp. J. 14 (2) (2008) 72–80.

[61] P. Dudek, FDM 3D printing technology in manufacturing composite elements, Arch. Metall. Mater. 58 (4) (2013) 1415–1418.
[62] S.C. Ligon, et al., Polymers for 3D printing and customized additive manufacturing, Chem. Rev. 117 (15) (2017) 10212–10290.
[63] M.J. Sauer, Evaluation of the Mechanical Properties of 3D Printed Carbon Fiber composites. Thesis, South Dakota State University, 2018.
[64] ASTM D570-98: Standard Test Method for Water Absorption of Plastics, ASTM International, West Conshohocken, PA, 2018.
[65] ASTM D4065: Standard practice For plastics: Dynamic Mechanical properties: Determination and Report of Procedures, ASTM International, West Conshohocken, PA, 2012.
[66] ASTM D7426-08: Standard Test Method for Assignment of the DSC Procedure for Determining Tg of a Polymer or an Elastomeric Compound, ASTM International, West Conshohocken, PA, 2013.
[67] M. Inoue, Studies on crystallization of high polymers by differential thermal analysis, J. Polym. Sci. Part A 1 (8) (1963) 2697–2709.
[68] B. Wunderlich, Thermal Analysis of Polymeric Materials, Springer, 2005.
[69] ASTM-D5477-18: Standard Practice For Identification of Polymer Layers Or Inclusions by Fourier Transform Infrared Microspectroscopy (FT-IR), ASTM International, West Conshohocken, PA, 2018.
[70] ASTM D790-07: Standard test Methods For Flexural Properties of Unreinforced and Reinforced Plastics and Electrical Insulating Materials, ASTM Inernational, West Conshohocken, PA, 2007.
[71] M. Eftekhari, A. Fatemi, Tensile, creep and fatigue behaviours of short fibre reinforced polymer composites at elevated temperatures: a literature survey, Fatigue Fract. Eng. Mater. Struct. 38 (12) (2015) 1395–1418.
[72] C.M. Agrawal, et al., Elevated temperature degradation of a 50: 50 copolymer of PLA-PGA, Tissue Eng. 3 (4) (1997) 345–352.
[73] K.R. Rajeesh, R. Gnanamoorthy, R. Velmurugan, Effect of humidity on the indentation hardness and flexural fatigue behavior of polyamide 6 nanocomposite, Mater. Sci. Eng. 527 (12) (2010) 2826–2830.
[74] R.A. Bubeck, E.J. Kramer, Effect of water content on stress aging of Nylon 6–10, J. Appl. Phys. 42 (12) (1971) 4631–4636.
[75] C.P. Kuda-Malwathumullage, Applications of Near-Infrared Spectroscopy in Temperature Modeling of Aqueous-Based Samples and Polymer characterization. Thesis, University of Iowa, 2013.
[76] S.S. Nair, C. Ramesh, Studies on the crystallization behavior of nylon-6 in the presence of layered silicates using variable temperature WAXS and FTIR, Macromolecules 38 (2) (2005) 454–462.
[77] S.J. Lue, et al., Diffusivity enhancement of water vapor in poly(vinyl alcohol)–fumed silica nano-composite membranes: correlation with polymer crystallinity and free-volume properties, J. Memb. Sci. 325 (2) (2008) 831–839.
[78] D.P. Russell, P.W.R. Beaumont, Structure and properties of injection-moulded nylon-6, J. Mater. Sci. 15 (1) (1980) 197–207.
[79] T. Isobe, et al., Comparison of strength of 3D printing objects using short fiber and continuous long fiber, IOP Conf. Ser. 406 (2018), 012042.
[80] R.R. Fernandes, A.Y. Tamijani, M. Al-Haik, Mechanical characterization of additively manufactured fiber-reinforced composites, Aerosp. Sci. Technol. 113 (2021), 106653.
[81] M. Ueda, et al., Three-dimensional printing of locally bendable short carbon fiber reinforced polymer composites, Adv. Industr. Eng. Polym. Res. 4 (4) (2021) 264–269.
[82] C. Ma, J. Faust, J.D. Roy-Mayhew, Drivers of mechanical performance variance in 3D-printed fused filament fabrication parts: an Onyx FR case study, Polym. Compos. 42 (9) (2021) 4786–4794.